Journal of Structural Geology, Vol. 14, No. 8/9, pp. 1101 to 1109, 1992
Printed in Great Britain

0191-8141/92 $05.00+0.00

Syndeformational grain growth: microstructures and kinetics

PAUL D. BONS*

Department of Earth Sciences, University of Utrecht, P.O. Box 80.021, 3508 TA Utrecht, The Netherlands

and

JANOS L. URAI

Shell Research BV, P.O. Box 60, 2280 AB Rijswijk, The Netherlands

(*Received* 3 *October* 1991; *accepted in revised form* 30 *March* 1992)

Abstract—Grain growth can be an important high-temperature process in fine-grained polycrystalline materials. We studied its effect on texture during deformation using a two-dimensional computer model and a see-through experiment with octachloropropane.

Syndeformational grain growth in geological materials can slow down the development of a grain shape preferred orientation or even obliterate it. Important processes are preferentially oriented deformation induced neighbour switches. The presence of a grain shape preferred orientation slows down the increase in grain size due to grain growth.

INTRODUCTION

GRAIN growth is usually defined as the recrystallization process in a polycrystalline aggregate which results in a reduction of free energy through reduction of the total grain boundary area (Smith 1964). In the absence of other processes this leads to a foam texture and to an increase in grain size. In other words growth of grains is a result of 'grain boundary energy driven grain boundary migration' (GBEGBM). Post-tectonic GBEGBM can cause partial or complete destruction of a microstructure, such as grain shape preferred orientation, if the tectonite was subjected to a high enough temperature for a long enough time after deformation. However, significant GBEGBM may well take place during deformation, for example during decreasing strain rates at the end of a deformation episode which overlaps with high-temperature metamorphism (Rutter & Brodie 1985).

The effects of GBEGBM during deformation have not yet received much attention, although several workers have mentioned it for playing a (minor) role during strain induced recrystallization (Urai *et al.* 1986, Knipe & Law 1987, Ree 1991). Deformation experiments on fine-grained wet quartz by Karato & Masuda (1989) have shown that grain size can increase considerably during deformation without the development of a grain shape preferred orientation (SPO). In metals the process has also been described to occur during high-temperature creep of superplastic alloys (Suery & Baudelet 1978).

In this study we investigated the effects of GBEGBM on SPO development during deformation, and the effects of deformation on GBEGBM. We developed a computer model to single out GBEGBM from other processes that modify the grain shape.

GRAIN BOUNDARY ENERGY DRIVEN GRAIN BOUNDARY MIGRATION: GBEGBM

Several workers used soap froth and oil emulsions as analogues for GBEGBM in polycrystalline solids (e.g. Smith 1964, Ashby & Verrall 1973). The thin fluid-films between the gas or liquid filled cells are interfaces with an associated interfacial tension. The cell walls move when material inside the bubbles diffuses through the walls. A minimum grain boundary energy is achieved (independently of the grain size) when all cell walls are straight and meet at 120°. Such an ideal arrangement, however, does not exist in nature, and natural foams or crystalline aggregates are therefore inherently unstable (Smith 1964).

The kinetics of GBEGBM can be described by:

$$(R - R_0) = k \cdot t^{(nd)}, \qquad (1)$$

where R is the grain size, R_0 is initial grain size, t is time, k is a constant and $n = 0.4$–0.5 (Olgaard & Evans 1986, 1988, Anderson 1988). The parameter, d, is dependent on grain size, R, and is 1 if R is grain radius, 2 if R is grain area and 3 if R is grain volume (Anderson *et al.* 1984, 1985). The process is also dependent on initial geometry or topology. If for example the starting material is ordered (e.g. contains many regularly shaped six-sided cells in two dimensions), growth will initially be slower (Glazier *et al.* 1987).

The growth process can be sub-divided into two sub-processes: equilibration of cell walls to achieve the lowest energy configuration, and growth of cells. In a soap froth the first sub-process takes place instan-

*Present address: Department of Earth Sciences, Monash University, Clayton, Melbourne, Victoria 3168, Australia.

taneously, because the walls and the contents of the cells (bubbles) have negligible strength, and the second sub-process takes place by material transfer through the walls. In a crystalline aggregate the cells (grains) are solid and both sub-processes have to take place by the time-dependent transfer of material across the grain boundaries (Weaire & Kermode 1984, Wejchert *et al.* 1986).

In real polycrystals, GBEGBM during deformation is always accompanied by the operation of deformation mechanisms (dislocation and diffusion) and usually also by other (dislocation driven) grain boundary migration processes. Although GBEGBM may be a significant microstructural process, its effects are difficult to study separately in experimental systems. For this reason we developed a computer model. Like many other workers we used a two-dimensional model, because the computer algorithms are simpler and Anderson *et al.* (1985) have shown that conclusions drawn from two dimensions are applicable to three dimensions (Weaire & Kermode 1983, Anderson *et al.* 1984, Srolovitz *et al.* 1984a,b, 1986, Grest *et al.* 1985, Soares *et al.* 1985, Wejchert *et al.* 1986, Glazier *et al.* 1987, Anderson 1988, Stavans & Glazier 1989).

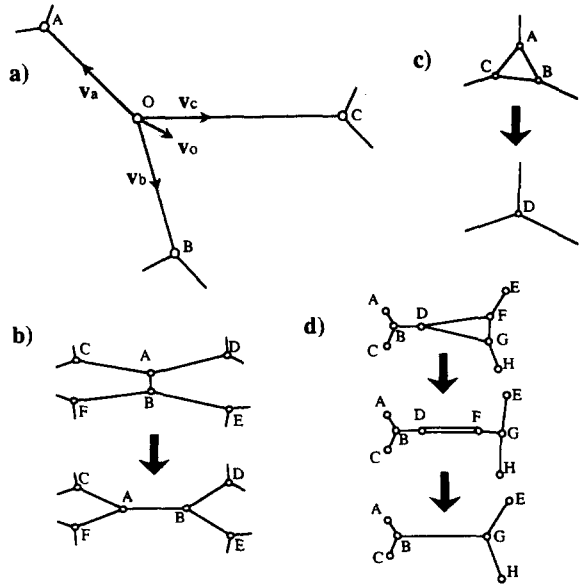

Fig. 1. Basic procedures of the model. (a) Movement of a triple junction, simulating GBEGBM. (b) Neighbour switching, or the *T*1 event. (c) Disappearance of an equidimensional three-sided grain, or *T*2 event. (d) Disappearance of a strongly elongated three-sided grain via a *T*1 event followed by the disappearance of a two-sided grain.

THE MODEL

Description

The model used in this study is a modification of the model of Soares *et al.* (1985). A two-dimensional polycrystalline aggregate is modelled as a network of straight grain boundaries that meet at triple junctions. Grain growth takes place by moving the triple junctions in small steps. Because grain boundary energy is the driving force, each triple junction has to move in a direction that reduces the summed length of the three joining triple junctions and thus reduces the grain boundary energy. In our model the movement vector ($\mathbf{v}_o$) of a triple junction is taken as the sum of the three vectors ($\mathbf{v}_a$, $\mathbf{v}_b$, $\mathbf{v}_c$) which are parallel to the three grain boundaries (Fig. 1a):

$$\mathbf{v}_o = \mathbf{v}_a + \mathbf{v}_b + \mathbf{v}_c. \quad (2)$$

The length of the three vectors is normalized to c, which is a user defined constant typically a few per cent of the average grain diameter. Thus

$$|\mathbf{v}_a| = |\mathbf{v}_b| = |\mathbf{v}_c| = c. \quad (3)$$

This has the effect that a triple junction will move towards a position where the three grain boundaries meet at angles of 120°.

To determine the movement distance of a triple junction in one time unit, one has to take into account the grain boundary mobility. The displacement $\mathbf{v}_o$ would cause the grain boundaries to sweep a certain area A, shown grey in Fig. 1(a). In our model the effect of grain boundary mobility is simulated by setting the maximum amount of material through which a grain boundary can migrate, i.e. the maximum swept area, in one time unit to a constant A_o. If A is larger than A_o, the length of $\mathbf{v}_o$ is adjusted according to

$$\mathbf{v}'_o = \frac{A_o}{A}\mathbf{v}_o. \quad (4)$$

This means that when A is small, either because the triple junction is almost in a stable position or the joining grain boundaries are short, the incremental triple junction movement is independent of the grain boundary mobility. When A is larger, the triple junction displacement is adjusted to take into account the limited rate at which grain boundaries can migrate through the material. The model is rather simple here, but the overall simplifications in the model do not justify a very elaborate modelling at this point. This adjustment of the displacement distance per time unit of a triple junction is the main difference between our model and Soares *et al.* (1985).

As the grains grow, the arrangement of grains changes: grains will change their number of sides and small grains will disappear. The basic topological changes to achieve this are called *T*1 and *T*2 events (e.g. Weaire & Rivier 1984).

T1 *event.* When one of the grain boundaries of a given triple junction becomes shorter than a user-defined minimum l_{min}, a neighbour-switch will occur (Fig. 1b). The grain boundary is replaced by a new grain boundary perpendicular to the old one and the triple junctions on either side will be rearranged. The length of the new grain boundary is set to a constant value (1.5) times the old length, to avoid reversal of the process during the next move of this triple junction.

Table 1. Conditions of the model simulations

Test	Number of moves (×1000)	Strain rate ($move^{-1}$)	Shear rate ($move^{-1}$)	Mean grain area at start	Mean grain area at end	Number of grains at start	Number of grains at end	c	l_{min}	R_a at start
0	100	—	—	799	2201	151	52	5	1	1.0
1	125	—	1.6×10^{-5}	404	731	315	168	1	1	1.0
2	500	—	4.9×10^{-6}	404	1741	315	68	1	1	1.0
3	125	8.0×10^{-6}	—	404	685	315	177	1	1	1.0
4	500	2.0×10^{-6}	—	404	1758	315	68	1	1	1.0
5	500	—	—	404	1718	315	72	1	1	1.0
6	350	—	—	404	894	315	131	1	1	4.0

T2 *event*. When a three-sided grain becomes smaller than a user-defined minimum, it disappears (Fig. 1c). The three triple junctions at its corners merge to one new triple junction. The criterion for a *T2* event to happen is that two of the grain boundaries merging at the selected triple junction are shorter than $2l_{min}$ and that these two GBs are boundaries of a three-sided grain. An elongated three-sided grain disappears in two steps (Fig. 1d). First it sheds its short side in a *T1* event, after which a two-sided grain remains. Its two triple junctions rapidly move towards each other until they have reached the threshold distance for a *T2* event, when the two-sided grain disappears. These two-sided grains are not visible in the graphic output of the model, because of the straight (and overlapping) grain boundaries.

During the simulation triple junctions are each randomly selected and moved according to equations (2)–(4), or altered by a *T1* or *T2* event. One selection and movement of a triple junction is defined to last one unit time. As the network is not periodic, some minor modifications are made for triple junctions at or adjacent to the network boundaries. Triple junctions can be displaced in small increments according to a user defined position gradient tensor, to model GBEGBM *during* deformation.

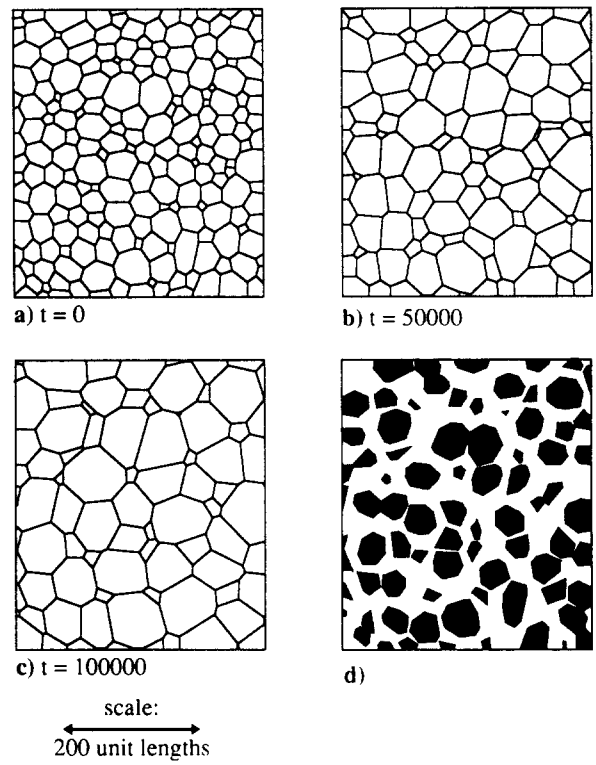

Fig. 2. Test 0: (a) starting material, (b) and (c) at time 50,000 and 100,000, respectively. (d) Unrecrystallized area (black) at t = 100,000.

Validity of the model

In the first of seven simulations (Table 1) we studied GBEGBM without deformation (Test 0, Fig. 2). The starting material was copied from a picture of a two-dimensional soap froth (Glazier *et al.* 1987, fig. 2b). During this run there was a three-fold increase in mean grain area and the total unrecrystallized area at the end of the run was 49%. This simulation was used to test the validity of the model, by comparing it with theoretical and empirical work presented by other workers (e.g. Anderson *et al.* 1984, Srolovitz *et al.* 1984b, Weaire & Kermode 1984, Glazier *et al.* 1987).

Figure 3(a) is a plot of grain area vs elapsed time. A growth-exponent (n in equation 1, with d = 2) of 0.5 can be fitted to the data.

According to Lewis's hypothesis, the normalized area of grains (grain area divided by average grain area) should remain a linear function of the number of sides of grains (Weaire & Rivier, 1984). Glazier *et al.* (1987) however found that Lewis's hypothesis does not hold for few sided cells in soap froth, and the same result was produced by the computer model of Weaire & Kermode

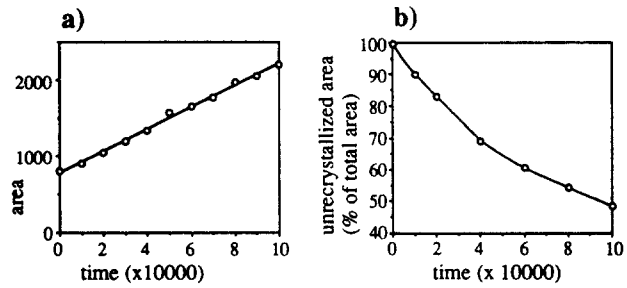

Fig. 3. Test 0: (a) average grain area as a function of time. The straight line is a linear fit through the data. (b) Percentage unrecrystallized area as function of time.

(1984). Figure 4(a) shows that Lewis's hypothesis is met for four- and more sided grains at t = 0 and t = 40,000 (151 and 89 grains, respectively, Fig. 4c).

According to Von Neumann's law (Von Neumann 1952), the growth rate of individual grains should be linearly dependent on the number of sides, and independent of time. Grains with more than six sides tend to grow, and grains with less than six sides tend to shed sides and shrink. Again this is shown for t = 0 and

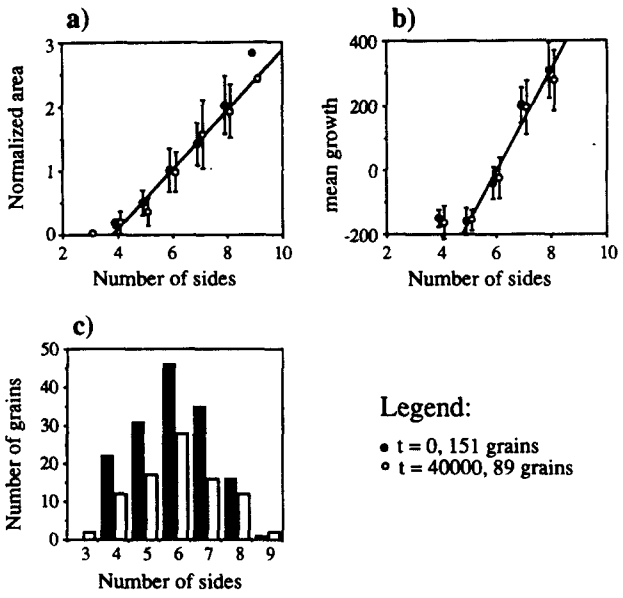

Fig. 4. Test 0: (a) normalized area of grains as a function of number of sides of grains. Straight lines are fitted through the data of four- to eight-sided grains. (b) Average increase in area as a function of number of sides. Straight lines are fitted through the data of five- to eight-sided grains. (c) Frequency of n-sided grains at $t = 0$ and $t = 40{,}000$. (Error bars are one standard variation in length.)

$t = 40{,}000$ (Fig. 4b). Here we see a deviation from theory: four-sided grains shrink more slowly than expected, and there are no measurements on three-sided grains. This is partly due to the measurement method, but also to the fact that grain boundaries are assumed to be straight in the model. For few and very many sided grains the error by this simplification becomes noticeable. In real crystalline aggregates and soap froths, three- and four-sided grains have boundaries with pronounced curvature, causing them to shrink faster than predicted by the model.

Except for the last point, the model appears to simulate GBEGBM well. Its accuracy is sufficient to demonstrate and illustrate the effects of GBEGBM during deformation. The model is indeed not designed to investigate accurately the details of GBEGBM itself.

GBEGBM during deformation

To simulate the effect of GBEGBM during deformation, the grain aggregate in the model was deformed in small increments during the simulation. We present the results of six simulations. Tests 1 and 2 are area-conservative simple shear at two different strain rates (Figs. 5b & c). Tests 3 and 4 are area-conservative pure shear (Figs. 5d & e). A fifth simulation (Test 5) is of GBEGBM without deformation, using the same starting material as for tests 1–4. Test 6 shows the effect of GBEGBM in an aggregate with a pre-existing grain shape preferred orientation. The starting material was the same as for the other tests (Fig. 5a), but deformed in plane strain up to a strain ratio of 4 (Fig. 5f).

Using the method described by Panozzo (1983, 1984), the average grain shape preferred orientation (SPO) can be described by an ellipse with an aspect ratio (R_a) and an orientation of the long axis of the ellipse (α). This ellipse was calculated at regular time intervals from the grain boundaries. Only grain boundaries that did not touch the network boundaries were used for the calculation. For comparison, the SPO development of the deforming starting material is calculated in the same way and plotted together with the results of the deformation simulations. The starting material had virtually no SPO ($R_a = 1.02$, $\alpha = 22°$).

It can be seen that there is a distinct lag in R_a development, the strongest at the lowest strain rates (Fig. 6). In the pure shear simulations α rapidly becomes perpendicular to the shortening direction, independent of strain rate. With simple shear α starts at 45° to the flow plane (line in two dimensions) and then rotates towards the flow plane. Only in Test 2 there seems to be a lag in rotation of α with respect to the maximum rotation speed. Up to $\gamma = 2.0$ the difference is hardly significant however.

The main reason that the simulations were not done to a higher finite shear strain was the fact that the model does not accurately describe the behaviour of small few sided grains. During deformation these will elongate disproportionally and introduce an error in the SPO measurements. Measured R_a values will therefore be too high and the rotation of α too fast. We are currently working on a modification of the model to correct for this effect.

The GBEGBM curve of Test 6 (Fig. 7a) shows an interesting effect. The rate of GBEGBM decreases with increase of SPO. The important factor is probably not the preferred orientation of all grains, but the fact that the individual grains are elongated, as in a Voronoi network (Soares *et al.* 1985, Wejchert *et al.* 1986). This effect was also obser-ed, but was less distinct, in an experiment with a two dimensional soap froth. The SPO decreased rapidly in Test 6 (Fig. 7b).

OCP EXPERIMENT

An annealed specimen of pure octachloropropane (OCP), mixed with marker-particles (26 μm), was deformed in pure shear to 23% shortening in a transmitted light deformation apparatus (see Urai *et al.* 1980, Means & Xia 1981, Means 1989 for description of experimental technique). Figure 8 shows the microstructure in a selected area, at three stages, together with a grid to display the finite deformation at those stages (see Jessell 1986 for method of strain analysis). Deformation was heterogeneous, which is a common feature of this kind of experiment.

A foam texture was largely preserved, indicating that GBEGBM was significant. Undulose extinction and the formation of large subgrains can be observed in several of the larger grains (see Ree 1991 for description of similar observations).

Twenty-seven $T1$ and several $T2$ events were observed. Some of these events are related because small four-sided grains disappear by a $T1$, followed by a $T2$

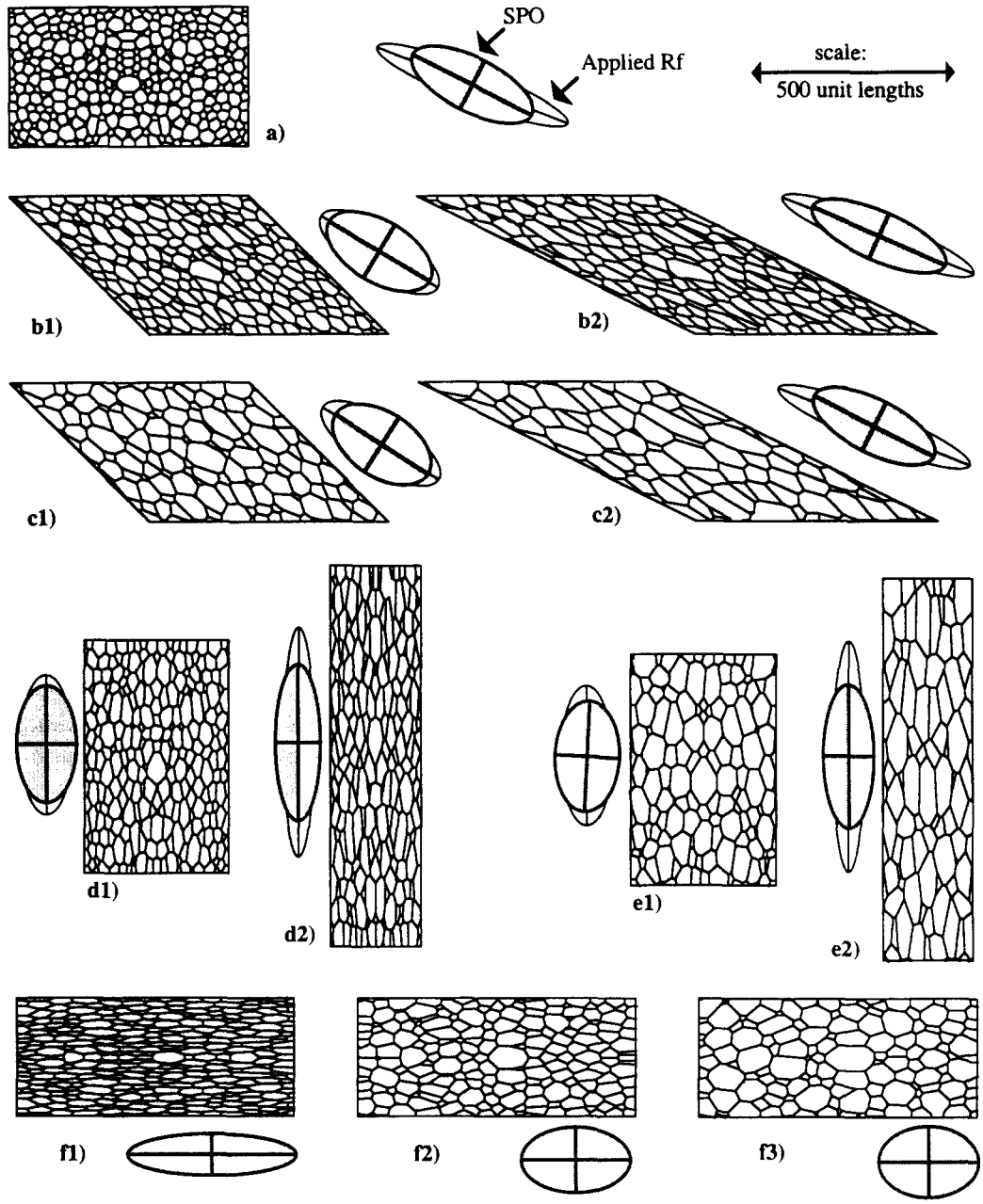

Fig. 5. Tests 1–4 and 6: GBEGBM during deformation. (a) Starting material. (b) Test 1: $\dot{\gamma} = 1.6 \times 10^{-5}$ at $t = 62{,}500$, $\gamma = 1.0$ (b1) and $t = 125{,}000$, $\gamma = 2.0$ (b2). (c) Test 2: $\dot{\gamma} = 4.0 \times 10^{-6}$ at $t = 250{,}000$, $\gamma = 1.0$ (c1) and $t = 500{,}000$, $\gamma = 2.0$ (c2). (d) Test 3: $\dot{\varepsilon} = 8.0 \times 10^{-6}$ at $t = 62{,}500$, $\varepsilon = 0.39$ (d1) and $t = 125{,}000$, $\varepsilon = 0.63$ (d2). (e) Test 4: $\dot{\varepsilon} = 2.0 \times 10^{-6}$ at $t = 250{,}000$, $\varepsilon = 0.39$ (e1) and $t = 500{,}000$, $\varepsilon = 0.63$ (e2). (f) Test 6: $t = 0$ (f1), $t = 250{,}000$ (f2) and $t = 500{,}000$ (f3). Open ellipses show finite strain ellipse and shaded ellipses the average axial ratio and orientation of grains. (b) and (c) are simple shear. (d) and (e) pure shear.

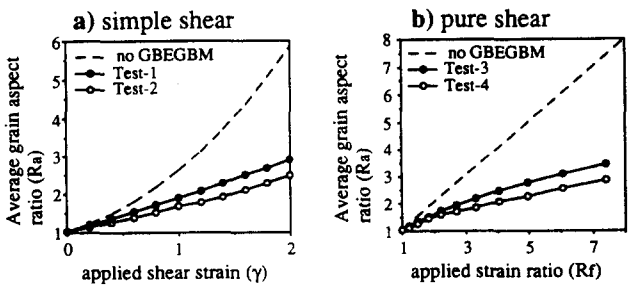

Fig. 6. Average grain aspect ratio (R_a) as function of applied strain ratio (R_f). (a) Simple shear tests. Tests 1 and 2. (b) Pure shear tests, Tests 3 and 4.

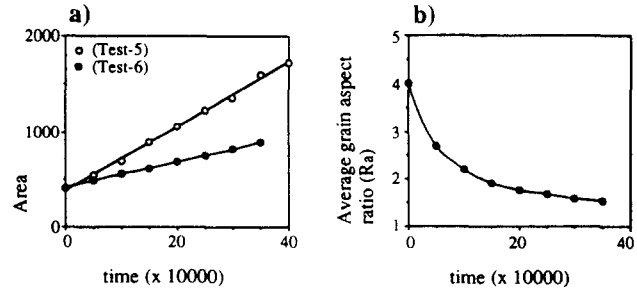

Fig. 7. Tests 5 and 6: average grain area (a) and average grain aspect ratio (R_a) (b) as a function of time.

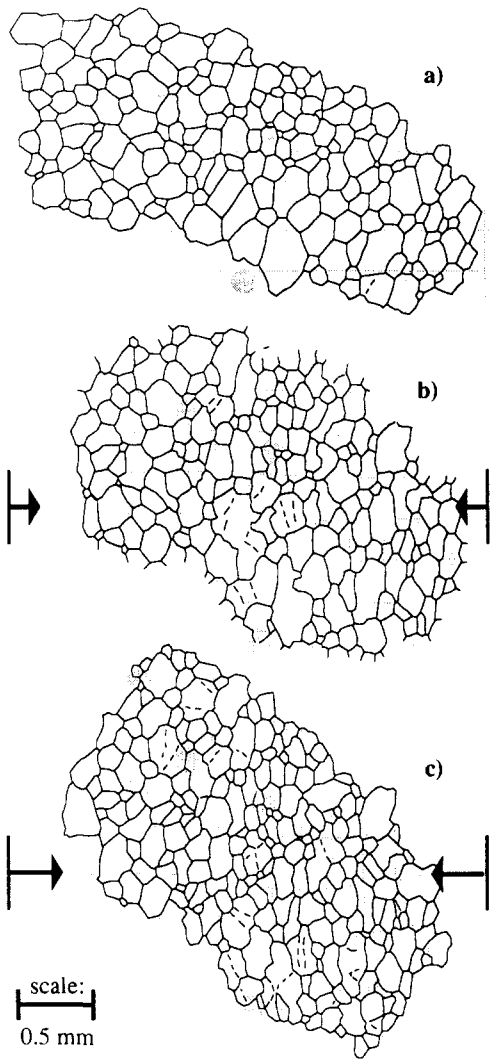

Fig. 8. Deforming polycrystalline OCP. The grid is drawn to depict the finite strain at each stage. (a) Starting material, (b) 11% bulk shortening, (c) 23% bulk shortening, in E–W direction. Shaded areas show positions of detailed drawings of Fig. 9.

event. Four $T1$ events are drawn in detail in Fig. 9. The $T1$ events have a strong preferred orientation with the newly formed grain boundaries preferentially perpendicular to the shortening direction. An R_a of 1.14, with the long axes of grains perpendicular to the shortening direction, was present at the start and increased to 1.33 at the end of the experiment, when the applied strain ratio was 1.7. This means that the R_a-increase lags significantly behind the applied strain ratio. These observations are very similar to those by Ree (1991).

DISCUSSION

Grain boundary energy driven grain boundary migration, GBEGBM, has two main effects that both influence the texture in a tectonite: increase of grain size and the decrease of SPO aspect ratio, R_a. Test 6 shows that there is also an effect of texture on GBEGBM: its rate will decrease when grains flatten. The net effectiveness of GBEGBM depends on the extent to which it can 'keep up' with deformation, and on the importance of other competing microstructural processes (e.g. Urai *et al.* 1986).

Comparison with natural rocks and geological strain rates

In order to make predictions about the importance of GBEGBM during deformation for rocks under geological conditions we need to know GBEGBM rates in natural rocks. These will vary widely for different minerals, temperatures, pressure, fluid pressure, impurity content, etc. We will restrict ourselves to one example: GBEGBM in a pure quartz aggregate at 600°C and $P_t = P_f = 3$ kbar, for which Tullis & Yund (1981) provide GBEGBM rates extrapolated from their experiments on very fine-grained quartz aggregates. They predict a grain diameter of 0.6 mm after 10^5 years and 2.3 mm after 10^6 years, starting with a grain size less than 100 μm. To compare these values with our simulations we will express these in the form of equation (1) for area, assuming that the growth exponent n is 0.5 (which is roughly in accordance with the experimental data presented by Tullis & Yund 1981, and is equal to the growth exponent in our simulations),

$$R = -0.15 + 1.4 \times 10^{-13} t \qquad (5a)$$

(t = time in seconds and R the area in mm^2).

In our simulations the growth function was:

$$R = 377.61 + 3.4 \times 10^{-3} t. \qquad (5b)$$

In order to calculate what strain or shear rates would be comparable to those used for the simulations we have to define the relative growth rate $\dot{R}$ at a given grain size:

$$\dot{R} = \frac{1}{R} \cdot \frac{\partial R}{\partial t} = \frac{k}{R} \qquad \text{if } n = 0.5 \qquad (6)$$

and the relative strain or shear rate

$$\dot{\varepsilon}/\dot{R} \quad \text{or} \quad \dot{\gamma}/\dot{R}. \qquad (7)$$

As the grain size increases, the relative strain rate will decrease, so we will only look at relative growth rate and relative strain rate at the grain size of the starting material, which is 9.0×10^{-6} in our simulation tests 1–4. The strain rates ranged from 2.0×10^{-6} (Test 4) to 1.6×10^{-5} (Test 1), giving relative strain rates of 0.22–1.8.

The following values give an impression of the strain rates for a quartz aggregate that are equivalent to these relative strain rates. For a grain diameter of 0.1 mm the shear rate of Test 1 would be 1.7×10^{-11} s^{-1} and Test 4 3.7×10^{-12} s^{-1}. For a grain diameter of 5 mm these values would be 1.2×10^{-14} s^{-1} and 1.5×10^{-15} s^{-1}, respectively. These values suggest that GBEGBM and its effects on the development of microstructures can be significant in fine-grained rocks at low strain rates under geological conditions. It should be stressed that it will then only be one of the operating processes.

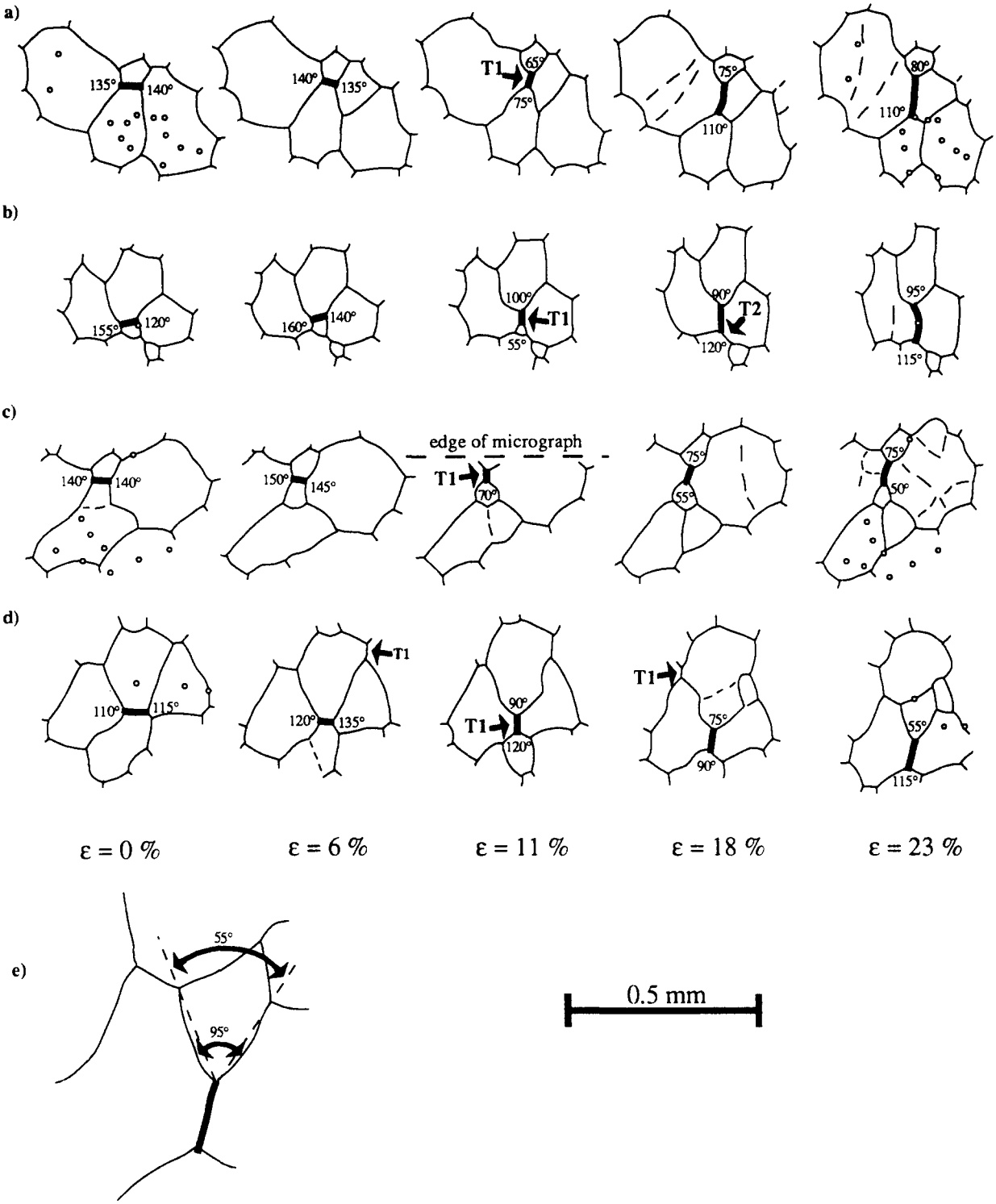

Fig. 9. (a)–(d) Selected neighbour switches or *T*1 events in the OCP experiment, taking place between 6 and 11% bulk shortening. The local grain boundary configuration is drawn for a bulk shortening of 0, 6, 11, 18 and 23%. Marker particles (if present) are drawn as small circles at 0 and 23% shortening. The numbers denote the opening angles (β) at the triple junctions. Note that these are on average larger than 120° before the switch and smaller after the switch. (e) Shows how the angle β is measured, taking into account that grain boundaries are usually curved. In the given case β is 55°.

Neighbour switching

Neighbour switching, or the *T*1 event, is a well known result of GBEGBM. Soares *et al.* (1985) pointed out that only those switches occur, whereby relatively few sided grains of the four involved lose one side and become detached. This rule fails for GBEGBM during deformation. This was observed by Ree (1991). This process is best illustrated with the ideal hexagonal geometry (Fig. 10), where all grain boundaries are stable and therefore do not migrate. The stable triple junctions A and B become distorted when the material is flattened. A and B will therefore move towards each other in order to regain a stable geometry. At a strain of 42.3%

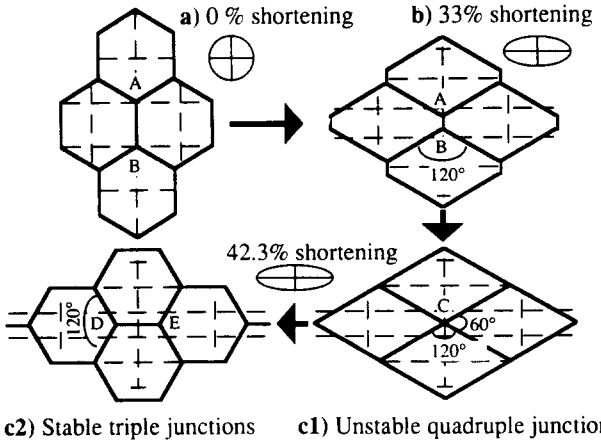

Fig. 10. Schematic drawing of strain-induced neighbour switching in two dimensions. The rectangular grid represents material lines.

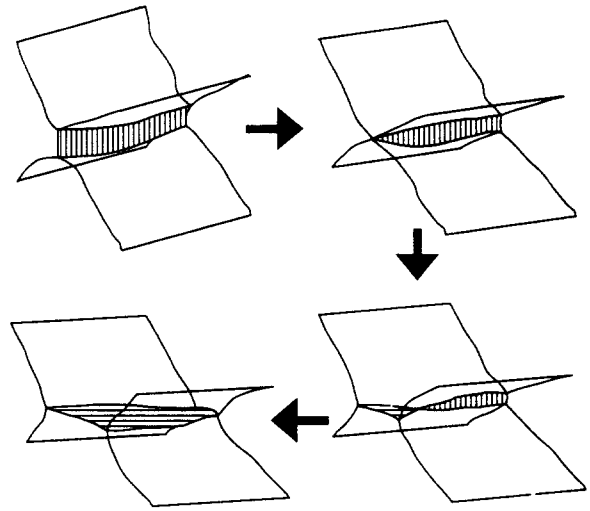

Fig. 11. Schematic drawing of strain-induced neighbour switching in three dimensions.

$(1 - \frac{1}{3}\sqrt{3})$ A and B merge into one quadruple junction, C. Because this quadruple junction has two 60° and two 120° angles it is highly unstable and will rapidly fall apart into two new triple junctions: D and E. D and E now move apart in directions perpendicular to the original movement direction of A and B. It is important to note that the grain boundary migration here is entirely due to distortions of the grain boundaries by deformation. Grain size remains constant and at 42.3% shortening all grains are equidimensional hexagons again.

A process giving similar textural developments, with an important contribution by neighbour switches, is (diffusion accommodated) grain boundary sliding (Ashby & Verall 1973). Although the actual flow of the material on the grain scale is completely different, these two mechanisms can (probably) not be distinguished using information on the resulting texture only. In two-dimensional see-through experiments they can be distinguished if enough markers are present in each of the grains involved in the neighbour switch. In the OCP experiment presented here there are only few signs of grain boundary sliding (Fig. 9d), but not enough markers are present to rule it out unambiguously.

Looking at the displacements of centres of grains, as was done by Ashby & Verrall (1973), is not a valid method to prove grain boundary sliding. Grain centres are determined from the grain boundaries, which are not material entities. The grain centres themselves are therefore not material entities and one needs to know the flow pattern of material points to prove grain boundary sliding (e.g. fig. 4 in Urai *et al.* 1986).

One difference between the two mechanisms are the angles (β) of grain boundaries joining at the ends of the grain boundary that is to be replaced during a neighbour switch (Fig. 9e). Taking the ideal geometry of equidimensional hexagons, β will remain 120° or increase if the neighbour switch is the result of GBEGBM and decrease to 90° if the switch is the result of sliding, using Ashby & Verrall's (1973) model. In the OCP experiment β was in most cases well over 120° before the switch (Fig. 9).

Going from two to three dimensions

So far we have considered a two-dimensional model. We will now briefly discuss the differences between the two- and three-dimensional case. The rate of increase of R_a will usually be lower in three dimensions than in two dimensions, and the observations in two dimensions have to be corrected for this. This is a simple geometrical correction, depending on the deformation (geometry) under consideration. Minimizing the grain boundary area in grain growth is achieved by forming equidimensional grains and by increasing the grain size. When a SPO exists the first process will be faster in three dimensions than in two dimensions, because the grain boundaries can move in one extra dimension to create equidimensional grains and thus lower the SPO. The dynamics of a neighbour switch will be similarly affected. In three dimensions a neighbour switch involves the disappearance of a two-dimensional interface between two impinging grains and the formation of a new interface perpendicular to the old interface (Fig. 11). The two impinging grains will first meet at one side of the disappearing interface, where that interface will lose one side and the new interface will form with initially three sides. If the old plane was (almost) stable with respect to the angles at which grain boundaries intersect at its sides, the new intersection angles will be unstable at the sides of the new plane (compare with Fig. 10) and this plane will grow rapidly at the expense of the old one. The effect is that a neighbour switch may happen relatively faster in three dimensions than in two dimensions.

From this we can draw some qualitative conclusions on the difference between three and two dimensions. The increase of R_a will usually be slower and the rate at which grain growth can lower an SPO is higher, so the development of an SPO will be even more slowed down by GBEGBM in three dimensions compared with two dimensions.

CONCLUSIONS

(1) Grain boundary driven grain boundary migration (GBEGBM) is a mechanism that can slow down the development of a grain shape preferred orientation (SPO) during deformation or even obliterate it.

(2) Deformation can induce extra neighbour switching, which decreases the development of a SPO.

(3) The increase in grain size because of GBEGBM is slowed down by the presence of a SPO.

(4) GBEGBM can be significant under conditions of low strain rate, small grain size and high temperature.

(5) The lack of a SPO at a small grain size is not sufficient to prove grain boundary sliding, but can be partly or completely the result of GBEGBM during deformation.

(6) These effects of GBEGBM during deformation can be observed in polycrystalline octachloropropane (OCP) deformed at high homologous temperature and low strain rate.

Acknowledgements—The authors are grateful to W. D. Means, A. Vauchez and B. Ph. van Milligen for their comments on the manuscript. Financial support to P. D. Bons by The Netherlands Organization for Scientific Research (NWO) is gratefully acknowledged.

REFERENCES

Anderson, M. P. 1988. Simulation of grain growth in two and three dimensions. In: *Annealing Processes—Recovery, Recrystallization and Grain Growth* (edited by Hansen, N., Jensen, D. J., Leffers, T. & Ralph, B). *Proc. 7th Int. Symp. on Metallurgy and Materials Science*, 15–34.

Anderson, M. P., Grest, G. S. & Srolovitz, D. J. 1985. Grain growth in three dimensions: a lattice model. *Scripta metall.* **19**, 225–230.

Anderson, M. P., Srolovitz, D. J., Grest, G. S. & Sahni, P. S. 1984. Computer simulation of grain growth—I. Kinetics. *Acta metall.* **32**, 783–791.

Ashby, M. F. & Verrall, R. A. 1973. Diffusion accommodated flow and superplasticity. *Acta metall.* **21**, 149–163.

Glazier, J. A., Gross, S. P. & Stavans, J. 1987. Dynamics of two dimensional soap froths. *Phys. Rev.* **A36**, 306–312.

Grest, G. S., Srolovitz, D. J. & Anderson, M. P. 1985. Computer simulation of grain growth—IV. Anisotropic grain boundary energies. *Acta metall.* **33**, 509–520.

Jessell, M. W. 1986. Grain boundary migration and fabric development in experimentally deformed octachloropropane. *J. Struct. Geol.* **8**, 527–542.

Karato, S. I. & Masuda, T. 1989. Anisotropic grain growth in quartz aggregates under stress and its implication for foliation development. *Geology* **17**, 695–698.

Knipe, R. J. & Law, R. D. 1987. The influence of crystallographic orientation and grain boundary migration on microstructural and textural evolution in an *S–C* mylonite. *Tectonophysics* **135**, 155–169.

Means, W. D. 1989. Synkinematic microscopy of transparent polycrystals. *J. Struct. Geol.* **11**, 163–174.

Means, W. D. & Xia, Z. G. 1981. Deformation of crystalline materials in thin section. *Geology* **9**, 538–543.

Olgaard, D. L. & Evans, B. 1986. Effect of second phase particles on grain growth in calcite. *J. Am. Ceram. Soc.* **69**, C272–C277.

Olgaard, D. L. & Evans, B. 1988. Grain growth in synthetic marbles with added mica and water. *Contr. Miner. Petrol.* **100**, 246–260.

Panozzo, R. 1983. Two-dimensional analysis of shape-fabric using projections of digitized lines in a plane. *Tectonophysics* **95**, 279–294.

Panozzo, R. 1984. Two-dimensional strain from the orientation of lines in a plane. *J. Struct. Geol.* **6**, 215–221.

Ree, J. H. 1991. An experimental steady-state foliation. *J. Struct. Geol.* **13**, 1001–1011.

Rutter, E. H. & Brodie, K. H. 1985. The permeation of water into hydrating shear zones. In: *Metamorphic Reactions, Kinetics, Textures and Deformation* (edited by Thompson, A. B. & Rubie, D. C.). *Adv. Phys. Geochem.* **4**, 242–250.

Smith, C. S. 1964. Some elementary principles of polycrystalline microstructure. *Metall. Rev.* **9**, 1–48.

Soares, A., Ferro, A. C. & Fortes, M. A. 1985. Computer simulation of grain growth in a bimodal polycrystal. *Scripta metall.* **19**, 1491–1496.

Srolovitz, D. J., Anderson, M. P., Grest, G. S. & Sahni, P. S. 1984a. Computer simulation of grain growth—III. Influence of particle dispersion. *Acta metall.* **32**, 1429–1438.

Srolovitz, D. J., Anderson, M. P., Sahni, P. S. & Grest, G. S. 1984b. Computer simulation of grain growth—II. Grain size distribution, topology, and local dynamics. *Acta metall.* **32**, 793–802.

Srolovitz, D. J., Grest, G. S. & Anderson, M. P. 1986. Computer simulation of recrystallization—I. Homogeneous nucleation and growth. *Acta metall.* **34**, 1833–1845.

Stavans, J. & Glazier, J. A. 1989. Soap froth revisited: dynamic scaling in the two-dimensional froth. *Phys. Rev. Lett.* **62**, 1318–1321.

Suery, M. & Baudelet, B. 1978. Rheological and metallurgical discussion of superplastic behaviour. *Rev. Phys. Appl.* **13**, 53–66.

Tullis, J. & Yund, R. A. 1981. Grain growth kinetics of quartz and calcite aggregates. *J. Geol.* **90**, 301–318.

Urai, J. L., Humphreys, F. J. & Burrows, S. E. 1980. *In situ* studies of the deformation and dynamic recrystallization of rhombohedral camphor. *J. Mater. Sci.* **15**, 1231–1240.

Urai, J. L., Means, W. D. & Lister, G. S. 1986. Dynamic recrystallization of minerals. *Am. Geophys. Un. Geophys. Monogr.* **36**, 161–199.

Von Neumann, J. 1952. Written discussion on grain topology and the relationship to growth kinetics. In: *Metal Interfaces*. American Society for Metals, Metals Park, Ohio, 108–113.

Weaire, D. & Kermode, J. P. 1983. Computer simulation of a two-dimensional soap froth—I. Method and motivation. *Phil. Mag.* **B48**, 245–259.

Weaire, D. & Kermode, J. P. 1984. Computer simulation of a two-dimensional soap froth—II. Analysis of results. *Phil. Mag.* **B50**, 379–395.

Weaire, D. & Rivier, N. 1984. Soap, cells and statistics—random patterns in two dimensions. *Contemp. Phys.* **25**, 59–99.

Wejchert, J., Weaire, D. & Kermode, J. P. 1986. Monte Carlo simulation of the evolution of a two-dimensional soap froth. *Phil. Mag.* **B53**, 15–24.